Sensors and Materials, Vol. 36, No. 10 (2024) 4343–4359
MYU Tokyo

S & M 3804

Research and Application of Hyperfine Realistic 3D Modeling Construction Based on Multisource Point Cloud Data

Chen Si,[1,2*] Bogang Yang,[1,2] Zengliang Liu,[1,2] Mengjia Luo,[1,2] Yongguo Wang,[1,2] Yingchun Tao,[1,2] and Xiaogang Zuo[1,2]

[1]Beijing Institute of Surveying and Mapping 60 Nanlishi Road, Beijing 100045, China
[2]Beijing Key Laboratory of Urban Spatial Information Engineering, 60 Nanlishi Road, Beijing 100045, China

(Received June 28, 2024; accepted October 16, 2024)

Keywords: terrestrial laser scanning, hyperfine realistic 3D model, point cloud data, urban components

At present, there are diverse data sources and mature technologies for the 3D modeling of cities, and 3D modeling is also developing towards component-level and refined modeling. In this study, we combined the needs of refined management in the central area of Beijing and elaborated on the practice of using various point cloud collection devices to carry out multisource point cloud data collection and ultrafine 3D modeling in areas where flight operations are not possible. There are three main areas of innovation: (1) the development of full-element ground acquisition and multisource point cloud joint 3D modeling technology, which solves the technical problems of acquiring all types of ground scanning data, such as those obtained using static, station-, cart-, backpack-, and vehicle-mounted laser scanning instruments, and handheld scanners, as well as multisource point cloud data fusion and modeling; (2) the development of a vehicle-mounted ultrahigh-resolution image acquisition system, which improves the efficiency of the vehicle scanner by increasing the exposure frequency to enhance its travel speed and (3) the use of tools to automatically extract urban components based on point clouds, which improved the efficiency of 3D modeling and achieved the fine-grained modeling of massive components in the region. On the basis of the system platform, the management and implementation of urban component-level information can be achieved.

1. Introduction

Currently, the 3D modeling data sources for cities are diverse and the technology is mature. For city-level 3D modeling, it is common to use methods such as piloting large aircraft or drones equipped with cameras to obtain oblique flight data for automated modeling, forming a realistic 3D model. For locally refined component-level 3D modeling, manual field photography, scanning, and other methods are often used to obtain texture and point cloud data. On the basis of point cloud data, 3D modeling and manual mapping are carried out. With the continuous upgrading of various laser point cloud acquisition equipment on the ground, the accuracy of laser point cloud data is high. As an important 3D modeling technology in the field of surveying,

*Corresponding author: e-mail: chensi2292@qq.com
https://doi.org/10.18494/SAM5208

ISSN 0914-4935 © MYU K.K.
https://myukk.org/

3D laser scanning technology provides a solution for high-precision and fine 3D model reconstruction.(1) In European and American countries, it is common to use laser scanning, oblique photography, and sonar depth measurement to generate high-precision 3D spatial data and to use professional visualization software to visualize and analyze a scene.(2) In China, there has been significant progress in research based on point clouds. Zheng *et al.*(3) proposed using a station scanning point cloud as the overall control network, with image dense matching point cloud and handheld fine point cloud as the main data sources, to carry out refined 3D modeling of grotto temples. Li *et al.*(4) achieved the high-precision 3D modeling of road infrastructure based on 3D vector and point cloud data. Zhang and Hou(5) used a vehicle-mounted laser measurement system to rapidly extract components such as main road poles, street lights, and ground signs. Zu(6) proposed a road parametric modeling method based on 3D laser point cloud.

The study area is located in the central urban area of Beijing. The current level of refinement of map elements is insufficient, and the abstract 2D map cannot fully meet the needs of real-world management. The existing technology cannot support the refined management of the region. In areas such as regional government support, emergency management, tourism services, and comprehensive environmental governance, hyperfine realistic 3D technology and data support are needed. However, the region is unable to obtain high-precision image data through aerial transportation for the construction of hyperfine 3D models. Therefore, we started with high-precision scanning equipment and carried out research and practical work.

2. Materials and Methods

2.1 Materials

We took the central area of Beijing as an example, using ground laser scanning equipment such as station-, cart-, backpack-, and vehicle-mounted laser scanning equipment to carry out high-precision point cloud data collection in the area, conducted ultrafine real-time 3D modeling, and implemented refined management methods and practices for urban component development systems.

2.2 Overview of technical methods

The method roadmap for hyperfine realistic 3D modeling based on high-precision point clouds proposed in this article is shown in Fig. 1. The overall route was divided into three parts: multisource data collection, the construction of hyperfine realistic 3D models, and the development of component management systems. Among them, in terms of multisource point cloud data collection, we explored the collaborative collection of point cloud data using equipment such as vehicle-, backpack-, ground-, and cart-mounted laser scanners. We analyzed the characteristics of laser point cloud data collected by various platforms, conducted research on rapid processing methods for multiplatform point clouds and methods for improving the accuracy of multisource point clouds, and formed a technical route for the collaborative acquisition and rapid processing of multisource dense point clouds. Combining high-precision

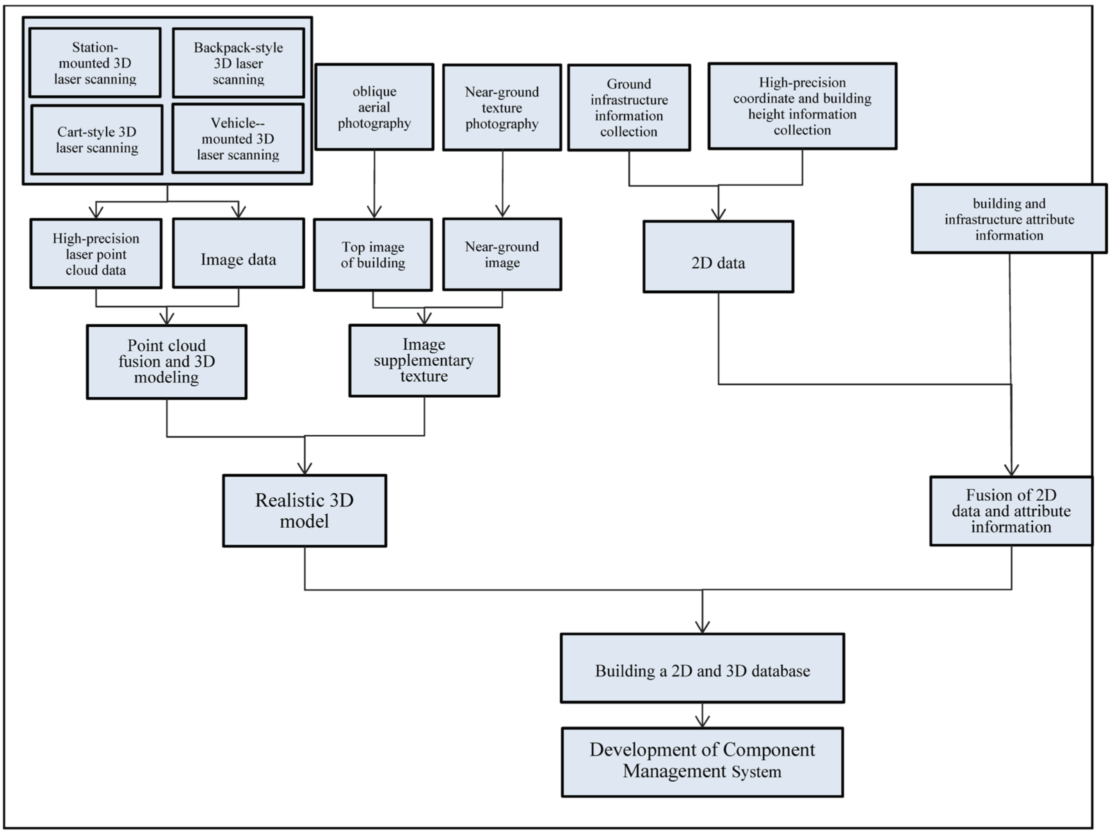

Fig. 1. (Color online) Overall technical roadmap.

point cloud data, we carried out 3D modeling for large buildings, cultural relics, roads, squares, and urban components. The image data captured by oblique aerial photography and the texture photos taken near the ground were used to supplement the texture of the top and bottom of the building. Multiple 3D modeling methods were used to achieve the hyperfine realistic 3D model construction of the area. Finally, combining 2D attribute information, we carried out 2D and 3D data linkage and database construction work and developed a system for urban component management based on the 3D Geographic Information System (abbreviated as “GIS”) platform to achieve the refined management of the region. The specific technical methods are described in detail below.

2.3 Multisource data collection

3D laser scanning technology is not limited by lighting, and using the principle of laser ranging, it can rapidly obtain dense spatial information on the surface of the measured object without touching it and generate a 3D point cloud model of complex scenes.[7] On the basis of the situation in the region, we used all terrain laser point cloud acquisition equipment such as static, station-, cart-, backpack-, and vehicle-mounted laser scanning instruments to obtain high-precision point cloud and image data (Fig. 2).

2.3.1 Regional overall accuracy control measurement

Owing to the use of four different types of scanning instrument and equipment for regional point cloud data collection, each device has a different data accuracy and status. To ensure consistency in data acquisition accuracy, secondary traverse points were set up in the survey area, and network observations were conducted at the beginning of the project. A total of 43 control points were set up, and four out of six GPS points were selected as known points for adjustment calculation in the plane control network. We selected two second-order leveling points around the survey area as known points of the elevation control network for adjustment calculation and completed a fourth-order leveling measurement of 10.6 km. The final elevation accuracy and plane accuracy errors are both within 5 cm, providing accurate control point data for subsequent point cloud data acquisition (Tables 1 and 2).

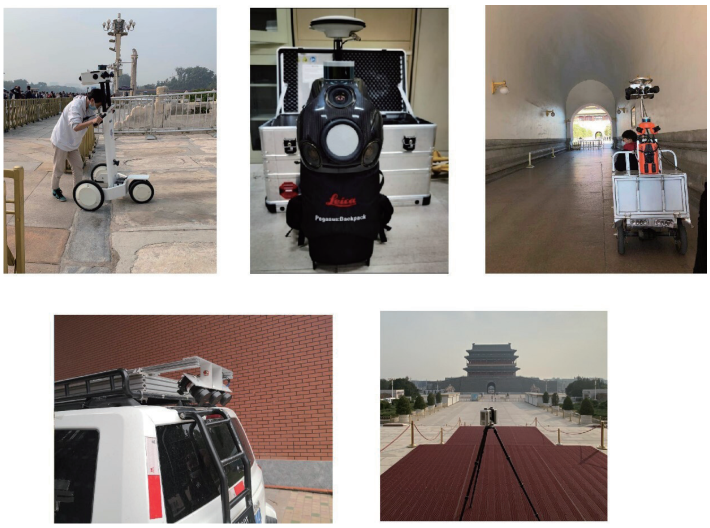

Fig. 2. (Color online) Schematic diagram of scanning site for various point cloud devices.

Table 1
Statistical table of mean square error in elevations.

Mean square error in elevation (mm)	$0 \leq m < 1$	$1 \leq m < 2$	$2 \leq m < 3$
Quantity	1	22	20

Table 2
Statistical table of plane error.

Mean square error in elevation (mm)	$0 \leq m < 1$	$1 \leq m < 2$	$2 \leq m < 3$
Quantity	18	20	1

2.3.2 Data acquisition of 3D laser scanner

1) Static 3D laser scanning

The static 3D laser scanning system consists of a laser scanner and a digital camera, and its operation method is similar to that of a total station.[8] In this study, we used the Leica RTC360 static station scanner, and the software uses Leica Cyclone Register 360 intelligent stitching software for point cloud denoising, correction, coloring, stitching, and other processing work. When collecting data from the Great Hall of the People and Chairman Mao Memorial Hall, the resolution should be intermediate (6 mm @ 10 m). When scanning small cultural relics such as an ornamental column and a lion sculpture, the resolution should be advanced (3 mm @ 10 m). The distance between stations should be within 15 m. At the same time, we designed scanning routes on the basis of the actual situation of the area to be scanned to ensure that the overlap rate of the scanned data meets the design requirements and achieve the high-precision stitching of the data through the reasonable placement of target positions. In the end, the static scanner scanned a total of 1196 stations with a data volume of 1.4 TB.

2) Cart-type 3D laser scanner data acquisition

The cart-type 3D laser scanning device, owing to its principle being different from that of traditional GPS positioning, can complete the work of many indoor and outdoor scenes with poor GPS signals,[9] and it is suitable for underground passages, pedestrian walkways, indoor areas, and so forth. This project uses the Navvis S465 cart-type 3D laser scanning system to collect data from four areas within the region, including underground passages, east–west pedestrian walkways of Tiananmen Square, national museums, and pedestrian walkways. The software uses SCENE for point cloud denoising, correction, coloring, stitching, and other processing tasks. Navvis Sitemaker is used for trajectory correction and point cloud processing, and an indoor viewer is used for browsing point clouds and panoramic images.

We reasonably planned the route on the basis of the on-site scanning range, reduced the drift error of the dataset trajectory, and improved the stitching accuracy by reasonably arranging anchor points [Fig. 3(a)] and overlaying them with the scanning common area [Fig. 3(b)], thereby obtaining high-quality point cloud and panoramic image data. The final data size is 105.8 GB.

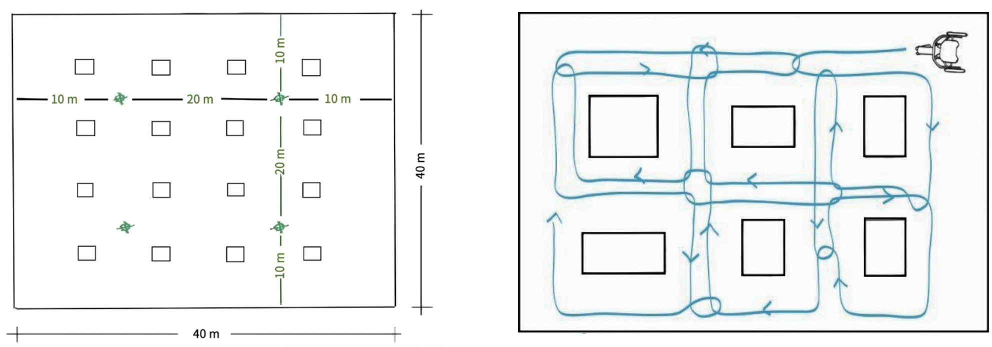

(a) (b)

Fig. 3. (Color online) (a) Anchor point layout diagram. (b) Scanning the overlay diagram of public area routes.

3) Backpack-style 3D laser scanner data acquisition

The backpack-style 3D laser scanner has the characteristics of high operational efficiency, rich information collection, and simple operation.[10] We used the Leica Pegasus Backpack mobile backpack scanner and Novatel InertialExplorer 8.70 software for trajectory processing. Leica Infinity software was used for data coordinate conversion, and Pegasus Manager software was used for point cloud processing. The main scanning areas include the surrounding areas of Tongzi River and the pedestrian walkway around the Great Hall of the People.

The scanning operation was carried out according to the route determined after site investigation. The camera shooting interval was set between 1 and 3 m according to the collection speed and modeling requirements. When the satellite signal was weak during the collection process (under bridges, tunnels, and so forth), the data was collected and stabilized until the satellite signal was good before continuing the scanning.[11] Finally, a total of 1.5 TB of data was obtained, including 120 GB of point cloud data.

4) Vehicle-mounted laser scanning data acquisition

Vehicle-mounted laser scanning has the characteristics of rapid data acquisition and the ability to obtain large-scale data in a short period of time, mainly used for the rapid reconstruction of road environments and urban street view building facades.[12] The vehicle-mounted mobile measurement equipment used in the project was the SSW vehicle-mounted laser modeling and measurement system independently developed by the China Academy of Surveying and Mapping Sciences.[13] It is a high-level measurement-oriented holographic 3D modeling mobile measurement system at home and abroad. The 3D coordinate accuracy of normal scanning within a hundred meter range is higher than 10 cm. In the case of a good GPS signal, the positioning accuracy plane is less than 10 cm, the elevation is less than 5 cm, and the precision road surface elevation measurement accuracy can reach 2 cm.[14] The vehicle-mounted laser scanner uses a modified high-resolution three-camera system to alternately capture ground data from Tiananmen Square and roads.

Before installation, the camera undergoes strict calibration to correct the distortion of the fisheye camera with a large field of view to a normal undistorted image (Fig. 4). A precise time synchronization control system can ensure the accurate matching of point clouds and images. We used the Sony A7 high-resolution camera to improve ground GSD, with an average ground GSD of 1.7 mm after modification. The highest high-resolution storage speed is 1 s per image, and it uses three cameras to alternate exposure, increasing it to 0.3 s per image. Under a 5 m exposure distance, the vehicle speed can be increased to 55 km/h, meeting the requirements for urban driving speed. Finally, the point cloud scanning work for TAM Square, Chang’an Avenue, the east–west side of the Great Hall, and Qianmen Street was completed.

2.3.3 Texture data collection

Texture data collection consists of two parts: one is based on oblique aerial photography to collect texture data on the top of buildings, and the other is to use full-frame mirrorless or single-lens reflex cameras to capture texture images of buildings and infrastructure. We utilized

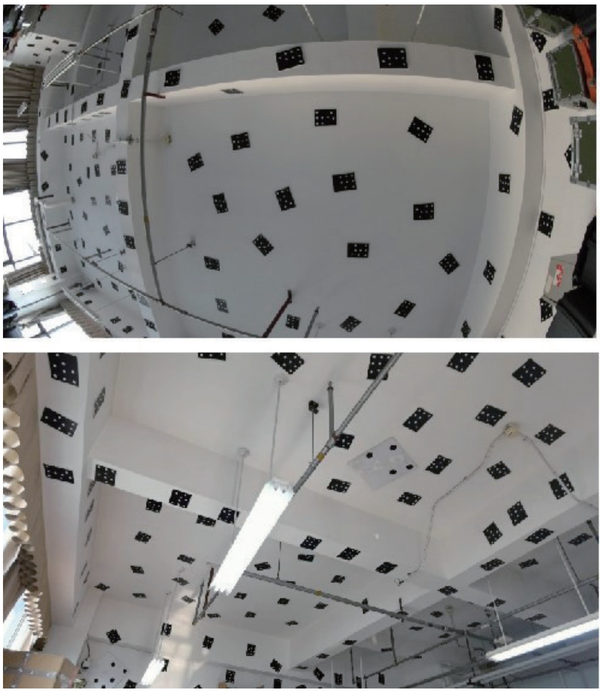

Fig. 4. (Color online) Schematic diagram of distortion correction for fisheye camera.

the data obtained from other oblique aerial photography, so the collection method and path are not described here.

Near-ground texture data shooting mainly collects buildings, structures, infrastructure, and so forth, which require texture mapping within the modeling area. When taking photos, we attempted to keep the camera's line of sight facing the surface to be photographed and paid attention to the angle between the camera and the surface to be not less than 70 degrees. When shooting, we chose an environment with soft lighting to avoid the effect of the environment on the color of the object being photographed and ensure the uniformity of texture and color in fine modeling.[15] When taking photos, we paid attention to the climate and lighting, and attempted to use forward or lateral forward lighting. Backlit photos are not suitable for use as texture photos.

2.3.4 Collection of infrastructure attribute information

The attribute collection of infrastructure mainly includes underground passages, public service facilities, lighting facilities, landscaping, landscape facilities, and monitoring facilities. By designing the structure of the above data content, each component of the same type of data is uniformly numbered, and specialized data such as accurate location, information description, height, width, and images are collected from the field for 3D modeling and management system database information storage in the office.

2.4 Construction of hyperfine realistic 3D models

2.4.1 Hyperfine 3D modeling of large buildings

Owing to the complexity of building facade composition, there is still significant room for improvement in terms of completeness, accuracy, and automation in current modeling methods.[16] The 3D model of important buildings is based on preprocessed laser point cloud data and manually modeled and mapped in 3ds Max. The resulting model meets the technical design specifications, as well as the requirements for scene operation efficiency and effect display. Overall, the prominent structures on important buildings, such as doors, windows, columns, eaves, decorative structures, and ancillary equipment, are made into solid objects (Fig. 5).

2.4.2 3D modeling of cultural relics

3D laser scanning can obtain a large amount of data on the surface of a building at a high speed, which can ensure the integrity of data on ancient buildings.[17] In this study, we used software programs such as Geomagic Wrap and Zbrush to automatically model cultural relics based on point clouds and photo textures with minimal manual intervention, highlighting the surface texture structure of cultural relics. We implemented texture-based automated mapping work and achieved the texture mapping of geometric models. Texture mapping is the process of mapping 2D images onto the surface of a 3D model, generating the necessary details for the model surface and restoring the textured material of the cultural relics themselves.[18] Modeling in this way is mainly for cultural relics in the region, mainly including stone lions, ornamental columns, and sculptures with complex structures (Fig. 6).

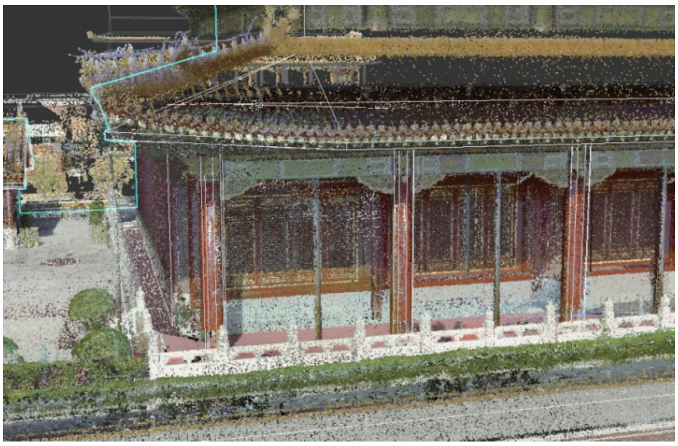

Fig. 5. (Color online) Schematic diagram of 3D modeling of stacked point clouds.

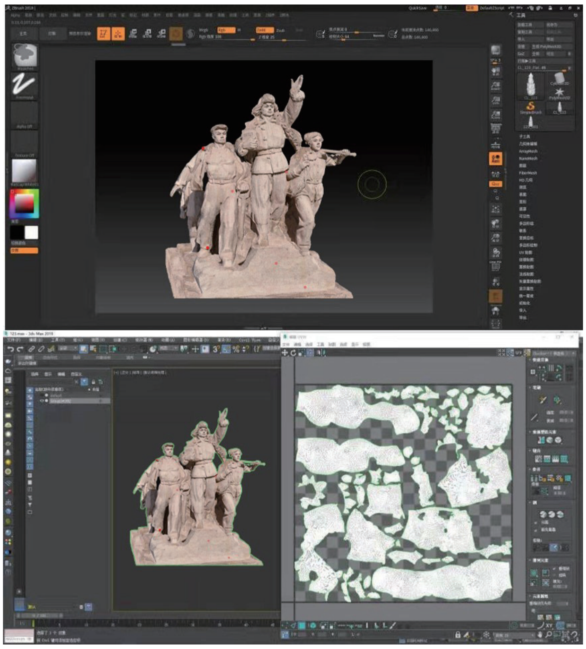

Fig. 6. (Color online) Schematic diagram of automatic 3D modeling of cultural relic sculptures.

2.4.3 3D modeling of urban components

The urban components in this study are mainly based on point cloud data for 3D modeling in 3ds Max, and texture mapping is performed using real photos. We studied different 3D modeling standards for different types of infrastructure. Facilities such as security cameras, lamp posts, and so forth are modeled in 3D according to the shape of the object to represent their structural features (Fig. 7). We used photo textures to represent the structural style of hollow facilities such as guardrails, which not only has high modeling efficiency and can express object features, but also reduces the load on 3D scenes.

2.4.4 3D modeling of urban roads and squares

Using a vehicle-mounted laser scanning system to scan and generate a 3D point cloud, we performed elevation anomaly filtering and batch rough classification, extracted ground and nonground points, achieved the efficient filtering of the point cloud, and generated a high-precision DEM.(19) We generated a 3D point cloud through the SSW vehicle-mounted laser scanning system, filtered the ground, and separated the ground point cloud for DEM modeling [Fig. 8(a)]. Then, distortion correction was applied to the photos taken by the camera, and the external orientation elements were obtained by combining the time synchronization system and POS data. Then, the photogrammetric method was used to project them onto the DEM, and finally, the complete road surface orthophoto was produced through tiling, uniform lighting, and color grading [Fig. 8(b)].

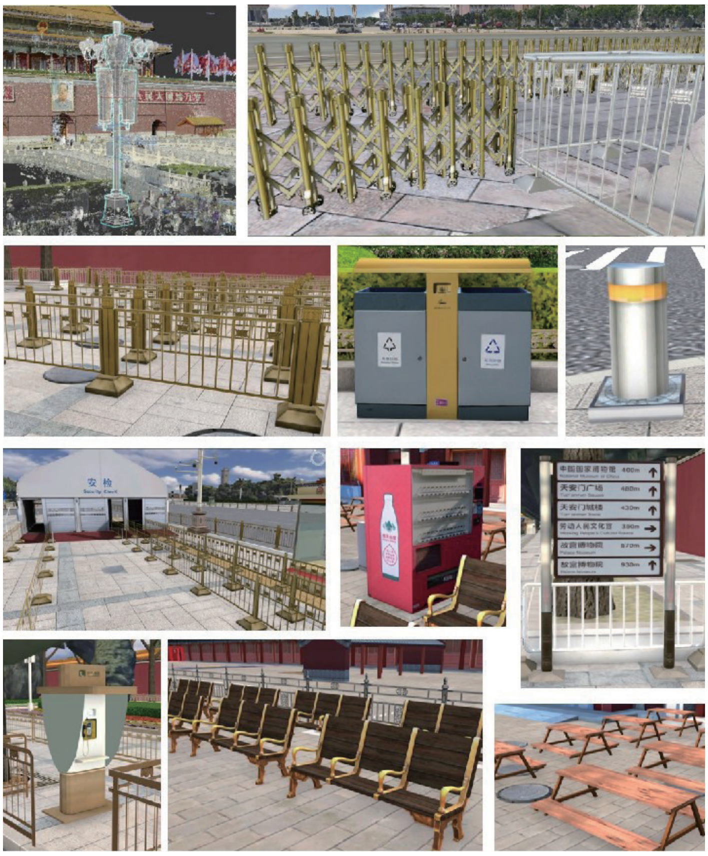

Fig. 7. (Color online) Schematic diagram of 3D model of infrastructure based on laser point cloud production.

(a) (b)

Fig. 8. (Color online) (a) Square ground orthophoto image. (b) Edited square ground orthophoto map.

This study is based on laser point cloud data and uses Tsinghua Shanwei software to extract the edges of more than 200000 floor tiles in the square. The elevation information of each tile corner point is entered, and the shp format tile vector surface data is output (Fig. 9). On the basis of the drawn shp vector data of the floor tiles, we examined the model for any broken surfaces, loss, distortion, stretching, or other issues. We created random textures with similar hues and clear textures. We used the program to randomly map textures onto the tile model and split the model by dividing multiple objects into regions. Finally, we baked the texture and generated a 3D model of the square that can pick up each tile (Fig. 9).

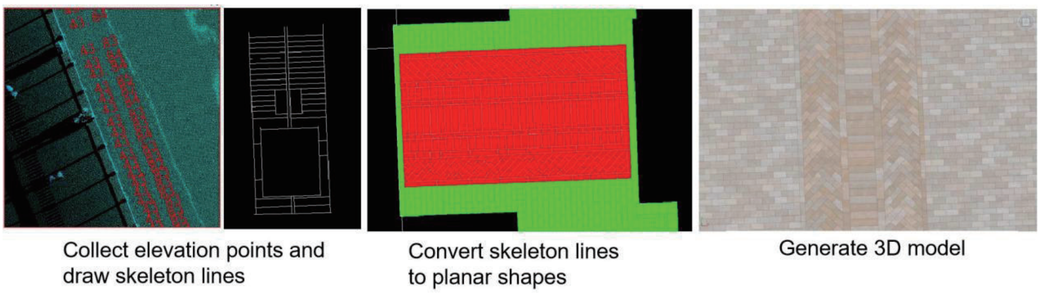

Fig. 9. (Color online) Schematic of production of 3D model of square floor tiles.

2.4.5 3D scene fusion

Finally, we integrated all the OSG and OSGB files of the 3D model data into CityMaker Builder for display. The scene data format is FDB, and the integrated model data can be used as a complete scene for display and application development. The scene integration uses preset offset values to ensure consistency with the coordinate system of the project design.

2.5 Design and implementation of infrastructure management system

2.5.1 System architecture

The system construction should be guided by the microservice concept, using Web Service technology as a means, combined with database technology and GIS graphic service engine, based on the CityMaker platform, to achieve resource and application system integrations under unified standards (Fig. 10). CityMaker is a mature and widely used domestic 3D GIS platform that provides excellent support for 2D and 3D GIS data, as well as BIM data from various platforms. Its performance is particularly outstanding in large-scale 3D scene rendering.(20) The system adopts a traditional three-tier architecture, with independent functions and low coupling between layers. Each layer is further divided into independent modules, encapsulated in components, to achieve separation between different modules, improve development efficiency, enhance system scalability, and improve system stability and maintainability.

2.5.2 System function implementation

The system carries various infrastructure and pipeline data in the region, and achieves the refined management of infrastructure through functional modules, such as spatial analysis, infrastructure query, infrastructure statistics, and infrastructure analysis, providing strong support for the management and planning of the region.

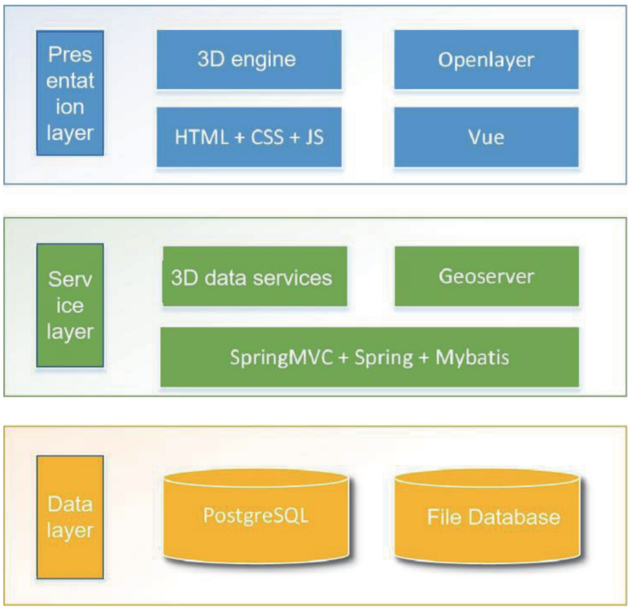

Fig. 10. (Color online) System architecture diagram.

3. Results and Discussion

3.1 Point cloud position accuracy detection and analysis

The absolute accuracy testing of the collected laser point cloud data is an important part of ensuring the effectiveness of point cloud data application in 3D model construction work. To accurately and effectively select the detection target point, we displayed the field measured data points in the sample graph. At the same time, on the basis of the description information of the measured points during field measurement, feature points were selected and collected using point cloud editing software.[21]

3.1.1 Statistics of plane position error

We collected 57 planar detection points within the sample area using GNSS RTK (Global Navigation Satellite System Real-Time Kinematic) or the total station, and compared their accuracies with the same named points in the point cloud data. Among them, there are two coordinate points where the terrain changes and they do not participate in the calculation. The actual number of planar detection points involved in the calculation is 55. We selected the coordinate points with more obvious features from the point cloud data, recorded the annotated coordinate x_i and y_i values, and found the corresponding feature points in the field. We used GNSS RTK to record the detection coordinate X_i and Y_i values, where n is the total number of selected coordinates. We calculated the mean square error according to Eq. (1).

$$M_S = \pm\sqrt{\frac{\sum_{i=1}^{n}[(X_i - x_i)^2 + (Y_i - y_i)^2]}{n}} \tag{1}$$

Referring to the accuracy requirements for first-level boundary points in the "Code for Land Surveying" (GB/T 42547-2023), which requires a point position error of no more than ±5.0 cm, we obtained the statistical results of planar position accuracy using 5 cm as the median error limit, as shown in Table 3. The selected feature points include building corners, poles, manhole covers, street lights, and signage, totaling 57 points.

3.1.2 Elevation error statistics

We collected 47 elevation detection points using GNSS RTK or the total station in the sample area and compared their accuracies with the same named points in the point cloud data. We selected the coordinate points with more obvious features from the point cloud data, recorded the annotated elevation coordinates h_i, and found the corresponding feature points in the field. We used GNSS RTK to record the detected elevation coordinates H_i, where n is the total number of selected coordinates. We calculated the mean square error according to Eq. (2).

$$M_n = \pm\sqrt{\frac{\sum_{i=1}^{n}(H_i - h_i)^2}{n}} \tag{2}$$

Referring to the accuracy requirements for first-level boundary points in the "Code for Land Surveying" (GB/T 42547-2023), which requires a point position error of no more than ±5.0 cm, we obtained the statistical results of elevation position accuracy using 5 cm as the median error limit, as shown in Table 4. The selected elevation feature points include building corner points, manhole covers, and marker lines, totaling 47 points.

Table 3
Statistical table of point cloud plane position accuracy.

Total number of coordinate points	57	Participate in calculation points	n = 55
$M_S = \pm\sqrt{\frac{\sum_{i=1}^{n}[(X_i - x_i)^2 + (Y_i - y_i)^2]}{n}}$	$\Delta \leq 0.05$	45	81.8%
	$0.05 < \Delta \leq 0.10$	10	18.2%
	$0.10 < \Delta$	2	3.6%
Precision type	0.05	Mean square error M	±0.04 m

3.2 Analysis of 3D model results

3.2.1 Evaluation of mathematical accuracy

In terms of mathematical accuracy testing, field inspection points are used to examine the accuracy of building 3D models and road models. The 3D model of infrastructure includes public service, lighting, and landscape facilities, as well as 3D models of trees and green spaces. Its placement should be consistent with the point cloud data, and mathematical accuracy evaluation is not required. According to the regulations of "Quality Inspection and Acceptance of Surveying and Mapping Results", when using high-precision data for accuracy detection, we selected coordinate points with obvious features from the 3D model data, recorded the annotated coordinate x_i, y_i, and z_i values, and found the corresponding feature points on site. We used GNSS RTK to record and detect the actual coordinate X_i, Y_i, and Z_i values, and calculated the error value of each coordinate. Using n coordinates, we calculated the mean square error according to Eq. (3).

$$M = \pm\sqrt{\frac{\sum_{i=0}^{n}\Delta_i^2}{n}} \tag{3}$$

In the formula, M is the mean square error of the results; N is the error in the detection point (edge); Δ is poor. After testing, the mathematical accuracy of the 3D model is as shown in Table 5. The mathematical accuracy of the 3D models of main buildings, squares, and roads is basically within 10 cm, meeting the accuracy requirements of urban 3D models.

3.2.2 Analysis of 3D scene integrity

The integrity of a 3D model is one of the key factors in evaluating its quality, which mainly includes the geometric integrity and surface texture integrity of the model.[22] In this study, we mainly examined the integrity analysis technique for the scene from the following aspects, namely, whether there is any interweaving, floating, or leaking between models in the scene; whether the relative relationship between the building and ground models is reasonable; whether

Table 4
Statistical table of point cloud elevation position accuracy.

Total number of coordinate points	47	Participate in calculation points	$n = 47$
$M_n = \pm\sqrt{\frac{\sum_{i=1}^{n}(H_i - h_i)^2}{n}}$	$\Delta \le 0.05$	46	97.9%
	$0.05\ \Delta \le 0.10$	1	2.1%
	$0.10 < \Delta$	0	0%
Precision type	0.05	Mean square error M	±0.03 m

Table 5
Statistical table of accuracy testing for 3D model results.

Category	Checkpoint (s)	Detection mean square error (m)
Building 1	17	0.081
Building 2	29	0.059
Building 3	8	0.074
Building 4	11	0.064
Square	18	0.081
Road	3	0.116

the overall color effect of the scene is coordinated; whether there are any stretching, distortion, or other issues with the texture; and whether there is any interweaving or leaking between the underground 3D model of the scene and the ground. After analysis, the 3D scene of this project has good integrity and presents good scene effect.

4. Conclusion

With the development and in-depth research of digital and smart cities, 3D urban components have received attention from all aspects as an important component of smart cities. The modeling and system construction of 3D urban components will become an important trend in the development of smart city management.(23) We explored the use of various types of ground laser scanning equipment to rapidly obtain point cloud data in a region. By controlling the accuracy of the data through unified measurement, ultrafine 3D model data of various buildings and urban components and facilities in the region were established. The research and development platform system realizes functions such as the attribute query, statistics, and measurement of various buildings and urban components. The establishment of the system platform provides precise real-time 3D data support for the preparation of large-scale events in the region. It plays an important role in the placement of various activity facilities, point simulation, attribute query, distance measurement, area calculation, and other aspects. It provides important support for the refined management of the region and has certain reference significance for the construction of smart cities.

Acknowledgments

Our research has received support from the Ministry of Science and Technology's Innovation Methods Work Special Project "Demonstration of Application of Innovative Methods in New Basic Surveying and Mapping Work".

References

1 P. Cheng, R. C. Zhang, and X. F. Yi: Proc. 2019 Jiangsu Society of Surveying and Mapping Geographic Information Annual Conf. (2019) 32. https://doi.org/10.26914/c.cnkihy.2019.043495
2 D. Wu, J. Li, D. B. Chou, and L. Y. Zhang: Surv. Spatial Geogr. Inf. **03** (2024) 61. https://doi.org/10.3969/j.issn.1672-5867.2024.03.018
3 G. Q. Zheng, G. S. Wang, and W. Z. Wang: J. Shandong Jianzhu University **04** (2023) 75. https://doi.org/10.12077/sdjz.2023.04.011

4 S. S. Li, B. Tian, and Z. Q. Hu: Highway Transp. Technol. S**1** (2022) 8. https://doi.org/10.3969/j.issn.1002-0268.2022.S1.002
5 L. L. Zhang and Y. Hou: Henan Sci. Technol. **06** (2018) 34. https://doi.org/10.3969/j.issn.1003-5168.2018.01.014
6 S. Zu: Urban Survey. **06** (2023) 70. https://doi.org/10.3969/j.issn.1672-8262.2023.06.016
7 Y. H. Chen: Research on 3D point cloud data processing technology based on laser scanning (University of Science and Technology of China, 2017).
8 F. Q. Chen: Geospatial Inf. **01** (2023) 140. https://doi.org/10.3969/j.issn.1672-4623.2023.01.029
9 H. R. Li: Research on SLAM Point Cloud Denoising Method and Modeling Route Optimization (Liaoning University of Engineering and Technology, 2023). https://doi.org/10.27210/d.cnki.glnju.2023.000633
10 S. Yue, D. J. Cai, W. H. Zhou, W. L. Xing, J. W. Shen, C. Y. Cui, and B. Q. Gao: Geospatial Inf. **07** (2022) 134. https://doi.org/10.3969/j.issn. 1672-4623.2022.07.031
11 H. Q. Xie, Y. T. Chen, and F. Zhao: Surv. Mapp. Bull. **02** (2019) 141. https://doi.org/10.13474/j.cnki.11-2246.2019.0061
12 M. L. Chen: Building extraction and geometric reconstruction based on multi station ground 3D laser scanning data (Wuhan University, 2018).
13 P. K. Zhang, L. Pei, and L. Z. Wang: Surv. Mapp. Sci. **09** (2015) 163. https://doi.org/10.16251/j.cnki.1009-2307.2015.09.034
14 X. Z Hou, Y. H. Wang, and J. Li: Surv. Spatial Geogr. Inf. **03** (2018) 167. https://doi.org/10.3969/j.issn.1672-5867.2018.03.052.
15 H. A. Zhong and H. Sun: Surv. Mapp. Bull. **12** (2023) 121. https://doi.org/10.13474/j.cnki.11-2246.2023.0370
16 P. Musialski, P. Wonka, amd D. G. Aliaga: Comput. Graphics Forum **32** (2013) 146. https://doi.org/10.1111/cgf.12077
17 L. W. Zhang, P. F. Liu, and G. Li: Beijing Surv. Mapp. **21** (2017) 68. https://doi.org/10.19580/j.cnki.1007-3000.2017.S2.018
18 G. Q. Zheng, G. S. Wang, and W. Z. Wang: J. Shandong Jianzhu University **04** (2023) 75. https://doi.org/10.12077/SDJZ.2023.04.011
19 X. J. Li and C. Y. Su: Resour. Guide **04** (2024) 26. https://doi.org/10.3969/j.issn.1674-053X.2024.04.019
20 H. Zhi: Geospatial Inf. **06** (2016) 22. https://doi.org/10.3969/j.issn.1672-4623.2016.06.007
21 S. P. Zhang, Y. C. Zhai, and L. Z. Wang: Surv. Mapp. Bull. **12** (2021) 110. https://doi.org/10.13474/j.cnki.11-2246.2021.383
22 A. Z. Hua and H. Sun: Surv. Mapp. Bull. **12** (2023) 121. https://doi.org/10.13474/j.cnki.11-2246.2023.0370
23 C. H. Yao and G. Chen: Surv Spatial Geogra. Inf. **05** (2020) 73. https://doi.org/10.3969/j.issn.1672-5867.2020.05.020

About the Authors

Chen Si received her master's degree in urban planning and design from the Beijing Institute of Architecture and Technology, China, in 2012. She is now a senior engineer at the Beijing Institute of Surveying and Mapping. Her research interests are in smart cities, geographic information, and real 3D construction. (chensi2292@qq.com)

Bogang Yang received his Ph.D. degree from Beijing Forestry University, China, in 2006, and he was engaged in postdoctoral work at Peking University from 2007 to 2009. Since 1983, he has been working at the Beijing Institute of Surveying and Mapping, and since 2004, he has been a professor-level senior engineer. He is the Director of the Beijing Key Laboratory of Urban Spatial Information Engineering. His research interests are in surveying and mapping technologies, smart city construction, and urban spatial analysis. (bogangy@126.com)

Zengliang Liu received his B.E. and M.S.E. degrees from China University of Mining and Technology, China, in 1999 and 2002, respectively. He is now a professorate senior at the Beijing Institute of Surveying and Mapping. His research interests are in 3D GIS, 3D modeling, and 3D laser scanning. (liuzengliang@bism.cn)

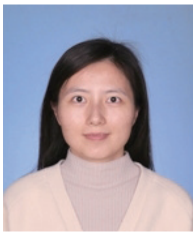

Mengjia Luo received her B.S. and M.S. degrees from Peking University, China, in 2010 and 2013, respectively. Since 2013, she has been an engineer at the Beijing Institute of Surveying and Mapping. Her research interests are in geographic information analysis and applications. (mengjia126@163.com)

Yongguo Wang received his M.S. degree in cartography and geographic information systems from Beijing Forestry University in 2012. He is now a senior engineer at the Beijing Institute of Surveying and Mapping. His research interests focus on surveying and mapping engineering, geographic information, and natural resource investigation. (wangyongguo@bism.cn) .

Yingchun Tao received her Ph.D. degree from Peking University in 2019. She is now a professorate senior engineer at the Beijing Institute of Surveying and Mapping. Her research interests are in new fundamental surveying and mapping, photogrammetry and remote sensing, and real 3D construction. (527359590@qq.com)

Xiaogang Zuo received his B.E. degree from the Beijing Institute of Architecture and Technology, China, in 2010. He is now a senior engineer at the Beijing Institute of Surveying and Mapping. His research interests are in basic surveying and new fundamental surveying and mapping. (zuoxiaogang999@126.com)